

APPENDIX A: SUPPLEMENTARY DATA

Table S1. Iron speciation based on Fe 1s XANES spectroscopy.

| Reference Species ^a | %Fe ^b | Fit Rank ^c | Observations | SPOIL ^c | Fe Valence | Class |
|--------------------------------|------------------|-----------------------|--------------|--------------------|------------|--------------|
| Major | | | | | | |
| ferrihydrite | 24 | good | 10 | 3.0 | III | oxyhydroxide |
| pyrrhotite ^d | 21 | good | 15 | 2.5 | II | sulfide |
| FeS ^e | 21 | fair | 8 | 3.4 | II | sulfide |
| pyrite | 16 | excellent | 12 | 0.8 | II | sulfide |

^a Reference Fe 1s XANES spectral database contains 60+ members (Marcus et al., 2008).

^b Percent Fe on a mole fraction basis is estimated by LCF fitting of Fe 1s XANES spectra (see section 2.4). The remaining ~18% of Fe is associated with minor, poor fit Fe(II) & Fe(III) species not reported.

^c Fit ranking is based on TTA subsequent to PCA, which generates a SPOIL suitability ranking: <1.5 excellent, 1.5-3.0 good, 3.0-3.5 fair, 4.5-6.0 poor (Malinowski, 1977; 1978).

^d Pyrrhotite includes polymorphs of varying stoichiometry ($\text{Fe}_{(1-x)}\text{S}$ $x = 0 - 0.2$). These observations include 4 of the FeS endmember also referred to as troilite (SPOIL = 2.4).

^e An unidentified, potentially amorphous, Fe monosulfide phase that appears to be distinct from both the pyrrhotite FeS endmember and mackinawite.

Table S2. Mn, Fe, Cu, and Zn sulfide and oxide mineralogy from X-ray diffraction data.

| Spot ^a | Sulfides | | | | Oxides | | | | Other phases |
|-------------------|---------------------------------|--|---|----------------------------|---|---|---|--|--|
| | Mn | Fe | Cu | Zn | Mn | Fe | Cu | Zn | |
| 0 | rambergite (MnS) | pyrrhotite (Fe _(1-x) S x= 0 – 0.2) | - | - | <i>hausmannite</i> (Mn ₃ O ₄) | <i>maghemite</i> (Fe ₂ O ₃) | - | - | <u>S₈</u> |
| 2 | - | mackinawite (FeS) <i>chalcopyrite</i> (CuFeS ₂) <i>villamaninite</i> (CuS ₂) | - | - | - | - | - | - | - |
| 3 | hauerite (MnS ₂) | mackinawite | - | - | - | - | - | - | - |
| 4 | <u>alabandite</u> (MnS) | - | cubanite (Cu _{0.33} Fe _{0.67} S) fukuchilite (Cu _{0.75} Fe _{0.25} S ₂) <i>chalcopyrite</i> | - | - | - | - | - | - |
| 5 | - | <i>greigite</i> (Fe ₃ S ₄) | <u>chalcocite</u> (Cu ₂ S) | - | - | - | <i>cuprite</i> (Cu ₂ O) | - | <i>Fe,</i> <i>native</i> |
| 6 | <u>alabandite</u> | - | <u>bornite</u> (Cu ₅ FeS ₄) cubanite | - | - | - | crednerite (CuMnO ₂) | franklinite ([Zn,Mn, Fe][Fe,Mn] ₂ O ₄) | <u>S₈</u> <u>S₆</u> |
| 7 | - | - | <u>covellite</u> (CuS) <u>bornite</u> | - | bixbyite (Mn ₂ O ₃) | - | <i>delafossite</i> (CuFeO ₂) | - | <u>S₈</u> |
| 8 | - | mackinawite pyrite (FeS ₂) | <u>chalcocite</u> (Cu ₂ S) cubanite <u>bornite</u> | - | - | - | - | - | - |
| 9 | - | - | - | <u>sphalerite</u> (ZnS) | - | - | - | - | - |
| 11 | - | - | <u>covellite</u> | - | bixbyite | - | - | - | <u>S₈</u> |
| 12 | - | - | cubanite | <u>sphalerite</u> | - | <u>magnetite</u> (Fe ₃ O ₄) | - | - | - |
| 13 | - | - | digenite (Cu _{1.95} S) | - | - | - | - | - | <u>S₈</u> |

Underlined minerals are consistent with geochemical modeling. Minerals in **bold** are consistent with major Fe bearing phases as identified by Fe 1s XANES. Minerals in *italics* are supported by just one peak in the XRD pattern.

^aLocations for X-ray diffraction data correspond to the spots indicated in Fig. 5a, spots 1 and 10 (not shown) had no identifiable XRD patterns.

Table S3. Additional 9°N regional endmember data for geochemical modeling^{a,b,c}.

| | Aa.3 | Aa.2 | Aa.1 | F.1 | L.1 | P.2 | Q.1 | P.1 | G.2 | C.1 | B.1 | G.1 | H.1 | D.2 | D.1 | E.1 | E.2 | K.1 |
|-------------------------------|------|------|------|------|------|------|------|------|------|------|------|------|------|------|------|------|------|------|
| T (°C) | 403 | 396 | 390 | 388 | 388 | 386 | 371 | 369 | 355 | 345 | 329 | 326 | 313 | 308 | 290 | 280 | 274 | 263 |
| pH ^d | 4 | 3.7 | 3.9 | 4.1 | 3.6 | 6.3 | 3.4 | 3.3 | 5.5 | 4 | 3.7 | 2.4 | 6.6 | 3.6 | 3.6 | 4.5 | 3.4 | 6.9 |
| O ₂ , aqueous | 0 | 0 | 0 | 0 | 0 | 0 | 0 | 0 | 0 | 0 | 0 | 0 | 0 | 0 | 0 | 0 | 0 | 0 |
| H ₂ , aqueous | 1 | 1 | 1 | 1 | 1 | 1 | 1 | 1 | 1 | 1 | 1 | 1 | 1 | 1 | 1 | 1 | 1 | 1 |
| SO ₄ ²⁻ | 1.9 | 1.6 | 0.5 | 0 | 0 | 0 | 0 | 0 | 0 | 0 | 0 | 0 | 0 | 0 | 0 | 0 | 0 | 0 |
| H ₂ S, aqueous | 82 | 66 | 34 | 37 | 68 | 47 | 29 | 25 | 20 | 9 | 7 | 16 | 16 | 6 | 10 | 9 | 6 | 6 |
| ΣCO ₂ , aqueous | 100 | 100 | 100 | 100 | 100 | 100 | 100 | 100 | 100 | 100 | 100 | 100 | 100 | 100 | 100 | 100 | 100 | 100 |
| Cl ⁻ | 43.3 | 30.5 | 80.9 | 46.2 | 114 | 178 | 71.4 | 135 | 154 | 329 | 416 | 150 | 371 | 801 | 846 | 859 | 841 | 556 |
| Na ⁺ | 40.3 | 26 | 71 | 35.6 | 99.9 | 174 | 61.9 | 114 | 137 | 288 | 359 | 132 | 332 | 671 | 707 | 708 | 703 | 464 |
| Ca ²⁺ | 1.06 | 1.45 | 2.00 | 1.34 | 2.21 | 6.93 | 0.81 | 1.17 | 0.20 | 11.9 | 17.1 | 1.53 | 7.08 | 41.8 | 45.5 | 46.9 | 41.8 | 23.0 |
| Mg ²⁺ | 0 | 0 | 0 | 0 | 0 | 0 | 0 | 0 | 0 | 0 | 0 | 0 | 0 | 0 | 0 | 0 | 0 | 0 |
| K ⁺ | 0.21 | 0.62 | 2.19 | 1.24 | 2.76 | 0 | 1.57 | 2.39 | 1.89 | 9.52 | 12.9 | 2.94 | 15 | 40.8 | 41.8 | 41.3 | 41.3 | 27.8 |
| SiO ₂ , aqueous | 2.73 | 3.82 | 7.07 | 6.00 | 6.04 | 4.06 | 7.45 | 8.70 | 6.46 | 19.0 | 19.3 | 8.45 | 17.6 | 20.4 | 21.0 | 20.0 | 19.8 | 19.2 |
| Fe | 0.8 | 0.7 | 1.6 | 1.4 | 1.7 | 5.9 | 1.5 | 4.2 | 1.4 | 3 | 3.4 | 2.4 | 0.5 | 2.2 | 2.3 | 2.9 | 2.7 | 0.4 |
| Mn ²⁺ | 0.08 | 0.1 | 0.24 | 0.17 | 0.11 | 0.14 | 0.19 | 0.18 | 0.17 | 0.4 | 0.56 | 0.25 | 0.3 | 0.81 | 0.79 | 0.86 | 0.85 | 0.31 |
| Cu ⁺ | 0.04 | 0.04 | 0.04 | 0.04 | 0.04 | 0.04 | 0.04 | 0.04 | 0.04 | 0.04 | 0.04 | 0.04 | 0.04 | 0.04 | 0.04 | 0.04 | 0.04 | 0.04 |
| Zn ²⁺ | 0.1 | 0.1 | 0.1 | 0.1 | 0.1 | 0.1 | 0.1 | 0.1 | 0.1 | 0.1 | 0.1 | 0.1 | 0.1 | 0.1 | 0.1 | 0.1 | 0.1 | 0.1 |
| Ba ²⁺ | 0.01 | 0.01 | 0.01 | 0.01 | 0.01 | 0.01 | 0.01 | 0.01 | 0.01 | 0.01 | 0.01 | 0.01 | 0.01 | 0.01 | 0.01 | 0.01 | 0.01 | 0.01 |

All concentrations in mmol/kg vent fluid.

^a Vent chemistry data from Von Damm (2000).^b Median dissolved CO₂,aq and H₂,aq from Proskurowski et al. (2008).^c Cu⁺, Zn²⁺, and Ba²⁺ from EPR 21° N (Von Damm et al. 1985).^d *In situ* pH calculated from pH measured at 25 °C.

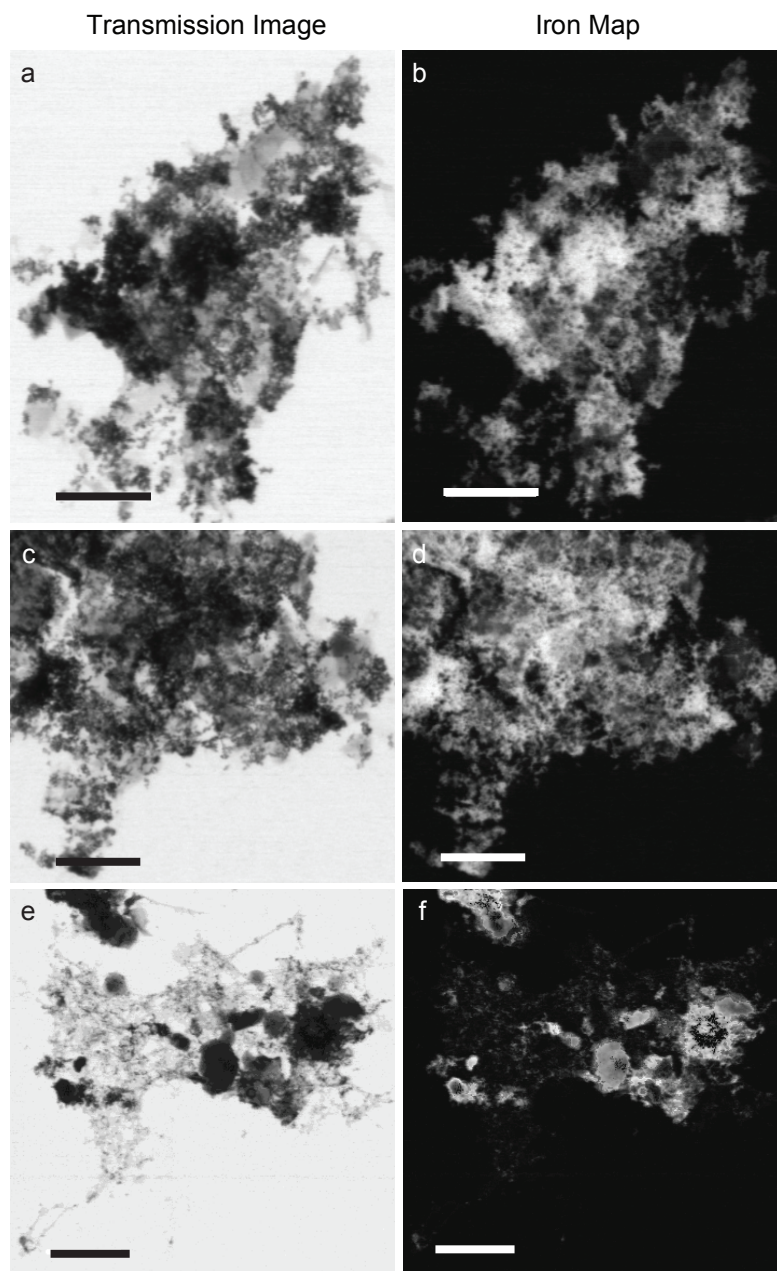


Figure S1. Examples of particle aggregation in nonbuoyant plume samples. Scanning transmission X-ray microscopy (STXM) images (a, c, e) and distributions of Fe (b, d, f). Scale bars for (a-d) are 2 μm . Scale bars for panels (e-f) are 5 μm .

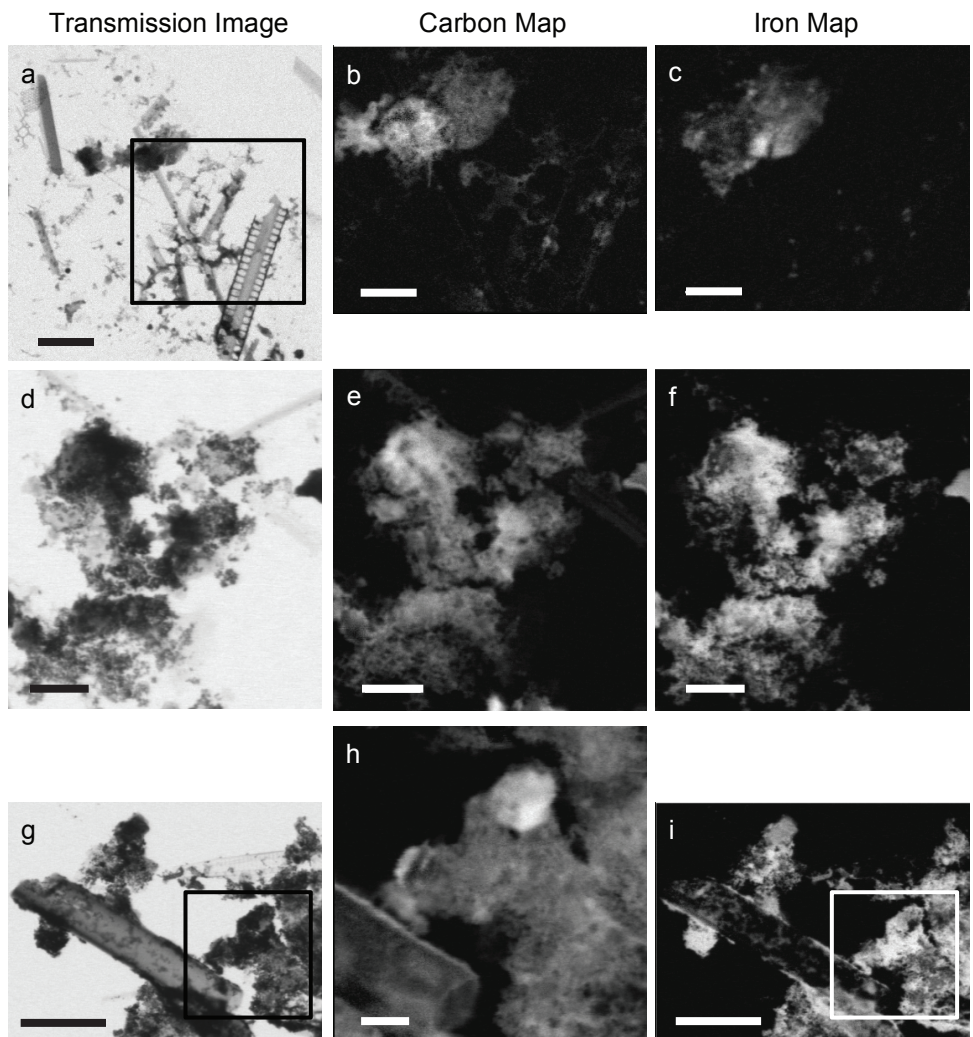


Figure S2. Examples of particle aggregation in plume samples. Scanning transmission X-ray microscopy (STXM) images (a, d, g), distributions of C (b, e, h), and Fe (c, f, i). Images in panels (a) and (g) are for samples from sediment traps (cruise and deployments described in Toner et al. 2009). The image in panel (d) is from this study (in situ filtration). All scale bars are 2 μm .

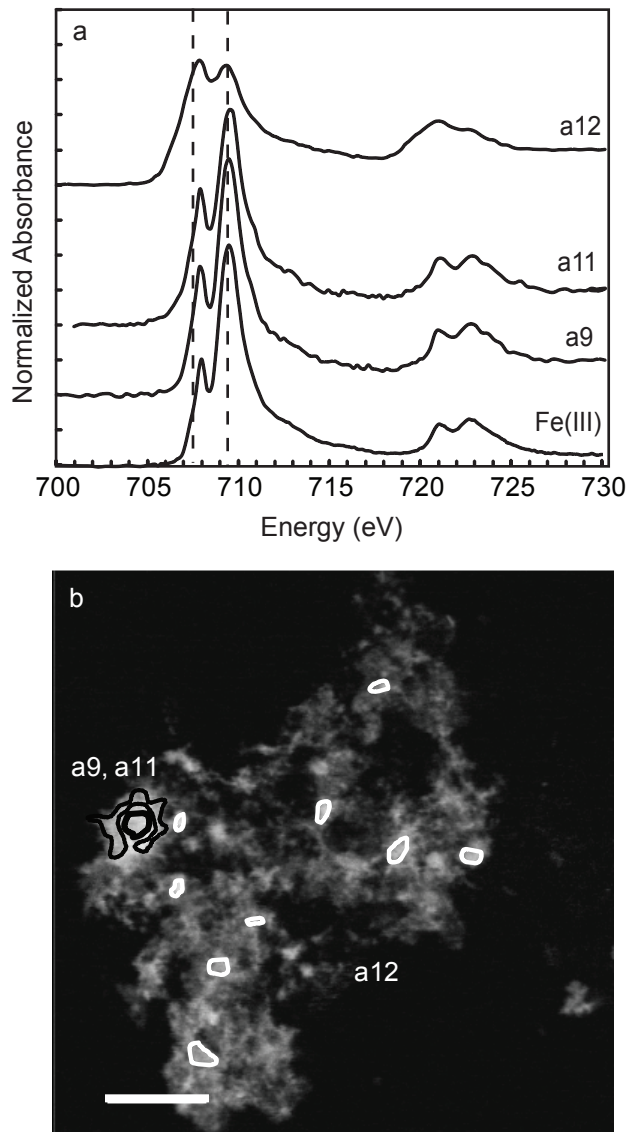


Figure S3. Speciation and spatial distribution of Fe in nonbuoyant plume aggregate. Iron 2p XANES spectra extracted from the STXM dataset are displayed in panel (a). The sample locations yielding the spectra are shown in panel (b); spectrum “a12” is the sum of the areas encircled in white. Scale bar is 2 μm . Vertical lines indicate Fe(II) at 707.6 eV and Fe(III) at 709.5 eV. The Fe(III) spectrum is a reference Fe(III) oxyhydroxide, ferrihydrite.

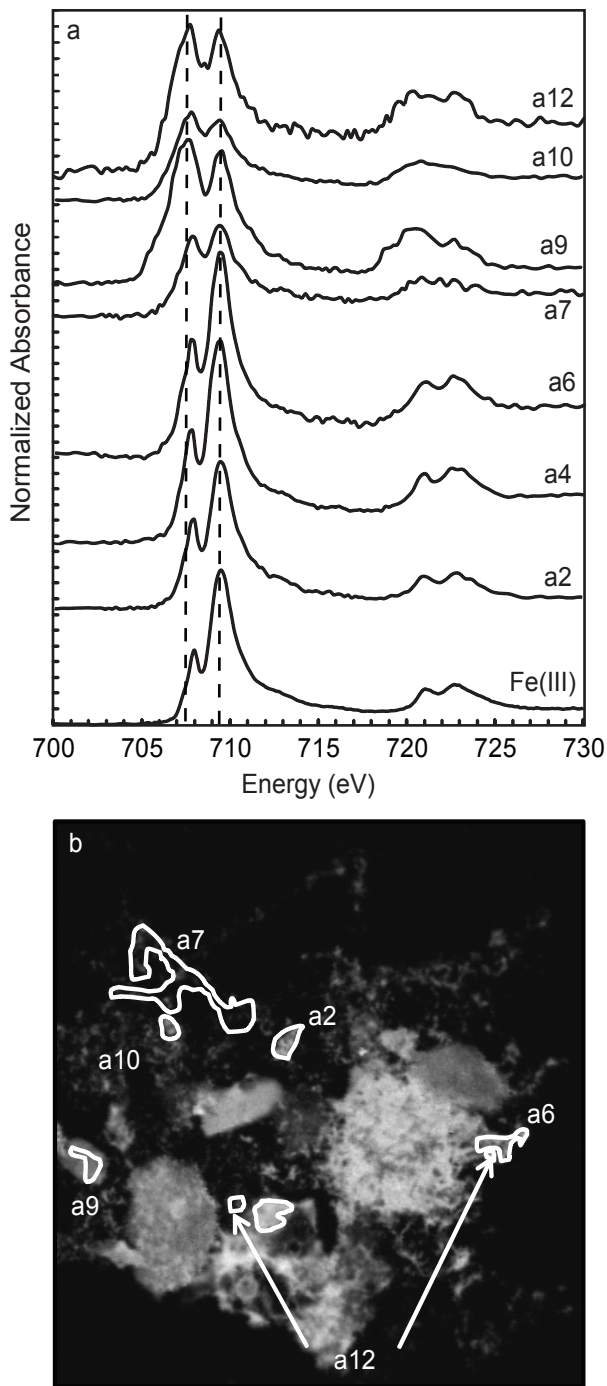


Figure S4. Speciation and spatial distribution of Fe in nonbuoyant plume aggregate. Iron 2p spectra extracted from the STXM dataset are displayed in panel (a). The sample locations yielding the spectra are shown in panel (b). Image (b) is 16 μm wide. Vertical lines indicate Fe(II) at 707.6 eV and Fe(III) at 709.5 eV. The Fe(III) spectrum is a reference Fe(III) oxyhydroxide, ferrihydrite.